



Effect of plasma treatment on the surface properties and antifouling performance of homogeneous anion exchange membrane

Zhijuan Zhao^{a,b}, Shaoyuan Shi^{a,b,*}, Hongbin Cao^{a,b,*}, Yuping Li^{a,b}

^aBeijing Engineering Research Center of Process Pollution Control, Environment Technology and Engineering Research Department, Key Laboratory of Green Process and Engineering, Institute of Process Engineering, Chinese Academy of Sciences, Beijing 100190, China, Tel./Fax: +86-010-82544844; emails: syshi@ipe.ac.cn (S. Shi), hbcao@ipe.ac.cn (H. Cao)

^bUniversity of Chinese Academy of Sciences, Beijing 100049, China

Received 21 January 2017; Accepted 29 August 2017

ABSTRACT

A homogeneous anion exchange membrane (AEM) with quaternary ammonium group was treated by low temperature plasma using different feed gases to improve the antifouling performance of AEMs in electro dialysis (ED). X-ray photoelectron spectroscopy analysis indicated that nitrogen- and oxygen-containing functionalities were incorporated, respectively, on the membrane surface after N₂ and O₂ plasma treatments. Scanning electron microscopy (SEM) and atomic force microscopy (AFM) analyses indicated that the surface morphology and surface roughness of the plasma-treated AEMs exhibited various changes because of the different etching effects of the two gases. Contact angle and zeta potential measurement confirmed that the surface hydrophilicity and negative charge density of the plasma-treated AEMs improved significantly and variously, which were related to the difference of the feed gases. No obvious changes occurred in the electrical resistance and ED performance of the plasma-treated AEMs, compared with the pristine AEM. The antifouling performance of the plasma-treated AEMs for sodium dodecylbenzenesulfonate (SDBS) improved significantly. Moreover, the O₂-treated AEM exhibited better antifouling property than the N₂-treated AEM. Results indicated that the high surface negative charge of the O₂-treated AEM was crucial to the improvement of the antifouling performance for SDBS.

Keywords: Anion exchange membrane; Plasma treatment; Antifouling performance; Electro dialysis; Surface properties characterization

1. Introduction

The membrane fouling of electro dialysis (ED), particularly the fouling of anion exchange membrane (AEM), significantly limits the extensive application of ED. Many foulants, such as humate, bovine serum albumin, and anionic surfactants, which have negative charges opposite to the surface charge of AEM, easily lead to the fouling of AEM [1–6]. Under an external electric field, foulants with negative charges move toward the AEM and are deposited on the membrane surface or enter the membrane channel because of the electrostatic interaction and affinity interaction between

the foulants and the membrane. Membrane fouling can cause an abrupt increase in electrical resistance, followed by an increase in energy consumption and a decrease in desalination efficiency. These effects significantly shorten the service life and increase the usage cost of AEM. Surface modification is an effective method to decrease the membrane fouling of polymeric membranes because of the changes in the properties of the membrane surface after modification [7–9].

Mulyati et al. [7,8] investigated the antifouling performance of AEM modified by the electrodeposition of polyelectrolytes on the membrane surface. Their findings showed that the electrodeposition of poly(sodium 4-styrenesulfonate) on the membrane surface could increase the negative charge density and surface hydrophilicity of AEM, which effectively reduced membrane fouling for

* Corresponding author.

sodium dodecylbenzenesulfonate (SDBS) [7]. Moreover, the different functional groups of the polyelectrolyte evidently affected the physicochemical properties and antifouling performance of the modified AEMs [10]. The polyelectrolyte layer was adsorbed on the membrane surface because of the electrostatic interaction and affinity interaction between the polyelectrolytes and the membrane. Thus, the antifouling performance of the modified membrane could be lost gradually because of the instability of the polyelectrolyte layer during ED. To improve the antifouling performance of the AEMs, particularly to increase the stability of the modified layer on the AEM, the other methods that modify the surface of AEM should be investigated further.

Plasma treatment effectively reduced the adsorption of foulants on the membrane surface by increasing the surface hydrophilicity of polymeric membranes, such as microfiltration membrane, reverse osmosis membrane, and nanofiltration membrane [9,11,12]. N_2 plasma treatment improved the filtration behaviors and flux recovery of the polypropylene microporous membrane, thus increasing the efficiency of membrane regeneration in a submerged membrane bioreactor; these outcomes were related closely to the formation of the functional groups on the membrane surface and the increase of surface hydrophilicity [12,13]. Different functional groups such as $C-O_x$ and $N=C$, $N\equiv C$ appeared on the membrane surface when the polyurethane membrane was, respectively, treated by O_2 or N_2 gas plasma [14]. The loss of the introduced groups and subsequent oxidation during storage in an aqueous environment occurred in the N_2 - and NH_3 -treated polyether urethane membranes; however, minimal change was observed for the O_2 - and Ar-treated membrane surfaces [15]. The results proved that the surface properties of the polypropylene microporous membranes could be changed differently by plasma gases, such as N_2 , O_2 , and NH_3 , a finding that indicated the chemical and morphological changes of the modified membrane surface are strongly influenced by the type of feed gas in the plasma treatment. The surface hydrophilicity of the polymeric membranes could be improved after plasma treatments using both N_2 and O_2 gases despite the differences of the etching effect and the incorporation of functional groups caused by the different types of feed gas [15–18], which might improve the antifouling properties of membranes. However, research about the plasma treatments of the AEM using N_2 and O_2 as the feed gases have yet to be reported.

In the present work, a homogeneous AEM with quaternary ammonium group (Neosepta AMX, Astom Corp., Tokyo, Japan) was modified by low-temperature plasma treatment using N_2 and O_2 as feed gas to improve the antifouling performance of AEMs in ED. The surface properties of the plasma-treated AEM were characterized by the measurements of X-ray photoelectron spectroscopy (XPS), SEM, atomic force microscopy (AFM), contact angles, zeta potential, and electrical resistance. The effect of plasma treatment on ED performance was also investigated by conducting a desalination experiment at a constant voltage. The antifouling performance of the plasma-treated AEMs was examined using SDBS as the model foulant in an actual ED system. In addition, the differences of the surface properties and antifouling performance of plasma-treated AEMs caused by the different feed gases were further analyzed.

2. Experimental

2.1. Materials

The AEM and cation exchange membrane (CEM) used in the experiment were Neosepta AMX and CMX (Astom Corp., Tokyo, Japan). The feed gases (O_2 and N_2) used for low-temperature plasma treatment had a purity of 99.99%. SDBS was purchased from Aladdin (Shanghai). Other reagents, such as NaCl and Na_2SO_4 , were analytically pure. Ultra-pure water (18.2 M Ω /cm, Milli-Q, Millipore, Germany) was utilized in all the experiments.

2.2. Plasma treatment of AEM

Low-temperature plasma treatment of the AEM was carried out with a plasma apparatus (CD-400MC, Europlasma, Belgium), which was driven by a 40 kHz radio frequency (RF) generator. The chamber was evacuated to a pressure of 60 mTorr before plasma treatment. The gas (O_2 or N_2) flowed to the chamber, and the flow rate was 32 mL/min. The working pressure was adjusted to 100 mTorr. The process of plasma treatment was all performed with the power of 200 W for a certain time. After plasma treatment, the membrane was taken out of the chamber and used to characterize the surface properties of the plasma-treated AEM and evaluate its antifouling performance.

2.3. Membrane characterization

The surface chemical composition of the AEM before and after plasma treatment was investigated by XPS using a 250Xi Escalab photoelectron spectrometer (Thermo Fisher Scientific, USA), which was used at the Al K α radiation (1,486.6 eV) unless otherwise stated. The survey and high-resolution spectra were obtained with pass energies of 100 and 20 eV, respectively. The C_{1s} peak at 284.7 eV was selected for energy calibration. The C_{1s} envelopes were analyzed and peak-fitted after the subtraction of a Shirley background using the Gaussian–Lorentzian peak shapes obtained from the Casa XPS software package.

The surface morphology of the membrane was observed by field emission scanning electron microscopy (FESEM; Hitachi SU8020, Japan) at an accelerating voltage of 5 kV and a current of 10 μ A.

The surface roughness of the membrane was characterized by AFM using Bruker Multimode 8 (Veeco, Germany) with a Nanoscope IV controller. The tapping mode was adopted to prevent damage to the membrane surface. The roughness (R_{ms}) value of the membrane was calculated using the software NanoScope Analysis.

The contact angle of the membrane was measured using a contact angle analyzer (OCA20, DataPhysics, Germany). A 5 μ L droplet was formed at a rate of 0.5 μ L/s on the membrane surface, and the contact angle was measured within 10 s by sessile drop method. The contact angle value was the average of five measurements on different places of each sample.

The zeta potential of the membrane was measured using a zeta potential measurement analyzer (Anton Paar, Austria). Two of the same membrane samples separated by a spacer were loaded into the clamping cell, and a channel was maintained for electrolyte flow. The zeta potential was measured by utilizing a 1 mM KCl solution (pH = 6.0) as the background electrolyte. The zeta potential value was the average of the

four measurements, including two in each flow direction (left to right and right to left).

The electrical resistance of the membrane was measured by an LCR Meter (NF2321, Japan) set at 100 kHz and 100 mV in 0.5 M NaCl at 25°C. The magnitude of impedance ($|Z|$) and the phase angle of impedance (θ) were measured with and without the membrane, respectively, and converted into the electrical resistance ($\Omega\text{-cm}^2$) value. The details were reported by Zhao et al. [19].

2.4. Electrodialysis performance

To examine the effect of plasma treatment on the performance of AEM in ED, the desalination experiment was carried out in an ED apparatus (Fig. 1), in which the titanium electrode coated by ruthenium and stainless steel electrode were used as anode and cathode, respectively. The ED stack contained one AEM (i.e., pristine AEM or N_2 plasma-treated AEM or O_2 plasma-treated AEM) and two CEMs (i.e., pristine CEMs). The stack was divided into three compartments, including the dilute, concentrated, and electrode compartments. The initial solution in the dilute and concentrated compartments was 500 mL of 0.1 M NaCl. The electrode rinse solution was 500 mL of the 0.1 M Na_2SO_4 . All the solutions were circulated through the dilute, concentrated, and electrode compartments and driven by a peristaltic pump at a flow rate of 100 mL/min. The ED experiment was performed at a voltage of 4.0 V. The electrical conductivity of the solution in the dilute compartment was measured by adopting a conductivity meter (S230, SevenCompact, Mettler Toledo).

2.5. Evaluation of antifouling performance

The antifouling performance of pristine AEM and plasma-treated AEMs was evaluated through the desalination

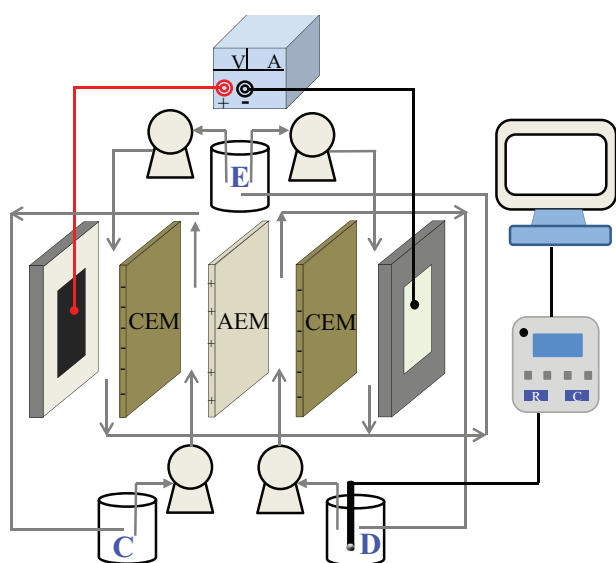


Fig. 1. Diagram of the electrodesalination experimental setup. CEM, cation exchange membrane; AEM, anion exchange membrane; C, concentrated solution tank; D, dilute solution tank; and E, electrode rinse solution tank.

experiment using the ED apparatus shown in Fig. 1. The details are described in section 2.4. The difference was that the solution in the dilute compartment contained 0.1 M NaCl and 50 mg/L SDBS as the model foulant. The electrical conductivity changes of the solution in the dilute compartment indicated the antifouling performance of the AEM.

To further evaluate the antifouling performance of the AEM, the fouling experiments were performed at a current density of 3 mA/cm². The apparatus was similar to that shown in Fig. 1. The 0.5 L solution composed of 0.1 M NaCl and 50 mg/L SDBS was flowed through the dilute and concentrated compartments, respectively, by the peristaltic pumps to the same beaker to ensure that the feed concentration was unchanged. The dilute and concentrated compartments were equipped with platinum plate electrodes to record the potential difference (ΔE) of the AEM using a data logger connected to a computer. When membrane fouling occurred, the potential difference increased gradually with time under the constant current because of the increase of electrical resistance. Thus, the change rate of the ΔE of AEM could reflect the antifouling performance of the AEM.

3. Results and discussion

3.1. Influence of plasma treatment time

In this work, the effect of the plasma treatment time on the properties of modified AEM was examined. The treatment time of AEM was set to 15 and 30 min for the N_2 and O_2 gases, respectively. The contact angle measurements of the plasma-treated membranes indicated that the contact angle value of the membrane treated with N_2 for 15 and 30 min was 43.9° and 35.5°, respectively, which meant that the longer treatment time was favorable in improving the hydrophilicity of N_2 -treated AEM. However, the electrical resistance of the membrane treated with N_2 for 30 min (4.40 $\Omega\text{-cm}^2$) was higher than that of the membrane treated with N_2 for 15 min (3.28 $\Omega\text{-cm}^2$), which could increase the energy consumption during the ED process. The contact angle of the AEM treated with O_2 for 15 and 30 min was 63.6° and 66.4°, respectively, which indicated that a long treatment time did not improve the hydrophilicity of O_2 -treated AEM. When the membrane was treated with 30 min using O_2 , the surface morphology exhibited obvious changes (Fig. 2), which could increase the surface roughness of O_2 -treated AEM. The result indicated that the membrane was etched severely under plasma treatment for a prolonged time period. Plasma treatment time could significantly affect the surface properties of the modified membranes, which was consistent with the result reported by Yu et al. [12]. Therefore, the plasma treatment time was determined to be 15 min in the succeeding work, and the surface properties and the antifouling performance of plasma-treated AEMs will be further examined.

3.2. Chemical composition of plasma-treated AEM

The XPS spectra were obtained to examine the chemical composition and the functional groups of AEMs. Fig. 3 indicates the high-resolution C_{1s} spectra of the pristine AEM, N_2 plasma-treated AEM, and O_2 plasma-treated AEM. Table 1 presents the chemical composition calculated

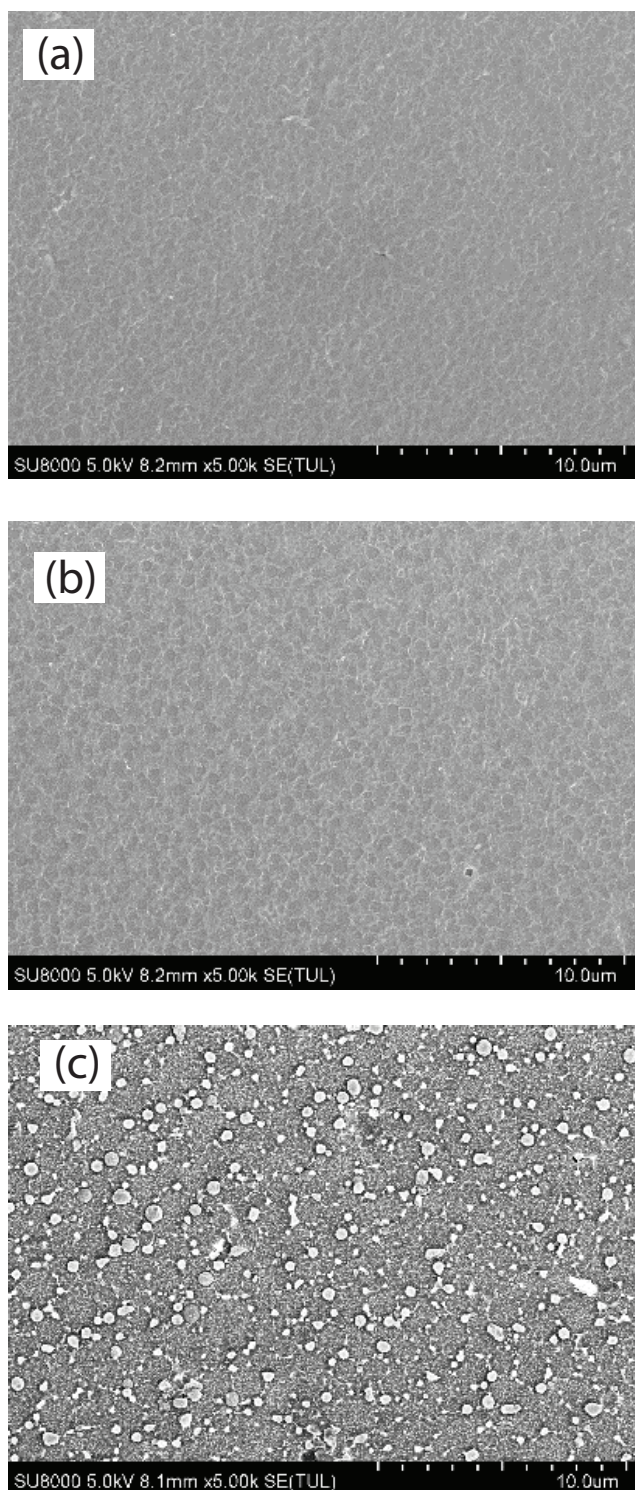


Fig. 2. SEM images with 5,000 \times of (a) pristine AEM and plasma-treated AEM using (b) N_2 and (c) O_2 for 30 min.

from the relative area of the XPS spectra. The C_{1s} spectrum of the pristine AEM (Fig. 3(a)) was fitted to the five peaks attributed to C–C (284.7 eV), C–H (285.3 eV), C–N (286.6 eV) in the quaternary ammonium groups, C=O (287.8 eV), and C=C (291.4 eV) of the aromatic ring in the membrane. It was

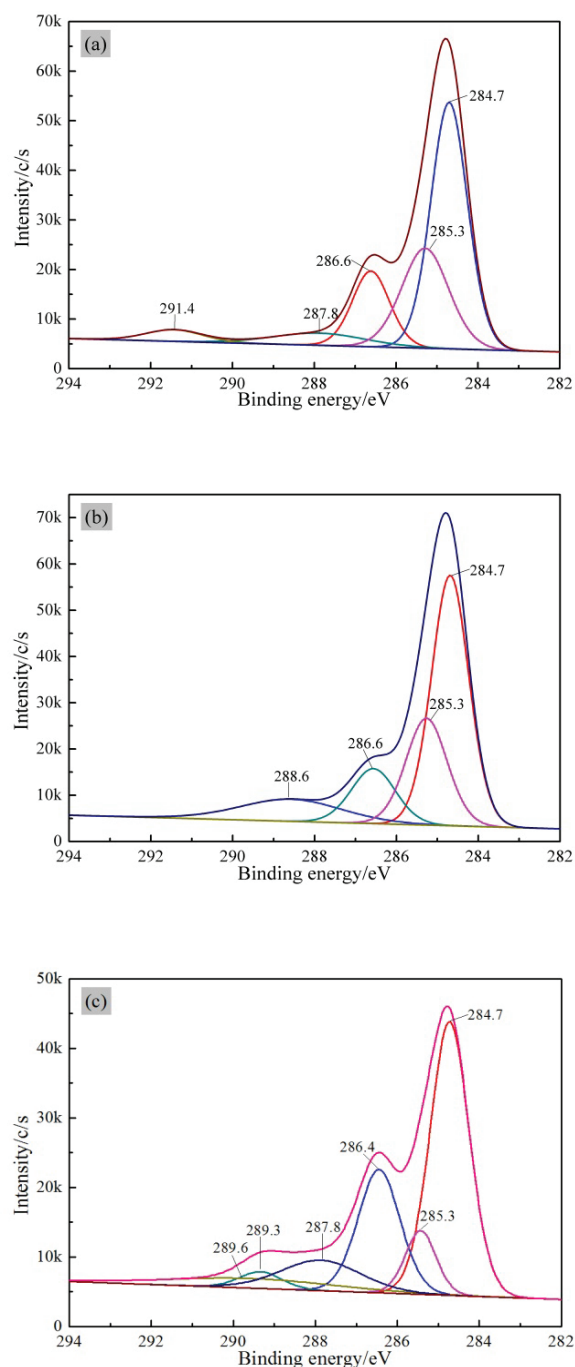


Fig. 3. High-resolution C_{1s} XPS spectra of (a) pristine AEM; (b) N_2 plasma-treated AEM; and (c) O_2 plasma-treated AEM.

reported that different species were detected in the N_2 plasma (such as N_2^+ , N_2^* , N, N^+ , and electrons) by optical emission spectroscopy [20]. These species could excite the membrane surface and cause the bond scission of the C–C (C–H) bonds. The activated membrane surface would react with the species from the N_2 plasma. The radicals (such as O^+ and O_2^+) produced by O_2 plasma could also react with the membrane and form new polar groups [21]. The polar groups formed by N_2 and O_2 plasma treatments would be analyzed qualitatively based on Figs. 3(b) and (c).

As shown in Fig. 3(b), after N_2 plasma treatment, the peaks at 284.7, 285.3, and 286.6 eV exhibited no obvious changes. This may be attributed to the high stability of several chemical bonds, such C–C and C–N or the incorporation of the $C-NH_x$ species, which could not change the shape of the peaks. However, the peaks at 291.4 and 287.8 eV disappeared, and a new peak at 288.6 eV appeared, which most likely resulted from the breaking of the double bonds C=C and C=O and the formation of imide. Moreover, as shown in Table 1, the atomic concentration of nitrogen increased to 3.58%, and the N/C ratio exhibited a slight increase; at the same time, the atomic concentration of oxygen increased to 17.13% and the O/C ratio increased from 0.17 to 0.23. The results indicated that the N_2 plasma treatment increased the concentration of both nitrogen and oxygen and the functionalization of nitrogen- and oxygen-containing species on the membrane surface. It was inferred that the certain functional groups on the surface of plasma-treated AEMs might disappear and new functional groups were formed when they were exposed to air, and the conversion process resulted from the instability of some species generated during plasma treatment and their tendency to be further oxidized by air [22–24]. Therefore, the oxygen content of the N_2 -treated AEM exhibited an obvious increase. Similar results (i.e., increasing nitrogen and oxygen content) were also observed by Weibel et al. [14] for polyurethane membrane treated with N_2 plasma.

As shown in Fig. 3(c), O_2 plasma treatment led to the variations of the peak intensities and peak positions on the XPS spectra of O_2 -treated AEM. It was observed that there was a large decrease in the hydrocarbon peak (285.3 eV) and significant increase in the carbon–oxygen binds, such as C–O (286.4 eV) and C=O (287.8 eV). In addition, several new peaks appeared on the spectra of O_2 plasma-treated AEM, which could be attributed to the formation of the ester/carboxyl groups (O=C–O at 289.3 eV) and carbonate group (O=C(–O) $_2$ at 289.6 eV) [25]. It was inferred that the scission of the C–C (C–H) bonds on the surface of the pristine AEM was easy to occur and the activated membrane surface would react with the oxygen species during the O_2 plasma treatment; therefore,

the ester/carboxyl functionalities might be formed and the formation of carbonate group might result from the further oxidation of the ester group [25]. Fig. 4 could be used to show the surface functionalization of the O_2 plasma-treated AEM. The XPS results demonstrated the different polar groups could be formed on the surface of N_2 -treated AEM and O_2 -treated AEM, which might cause the various changes in the physicochemical properties of the AEM to some extent. As shown in Table 1, the O/C ratio of O_2 -treated AEM increased from 0.17 to 0.32, which was caused by the surface functionalization of the O_2 plasma-treated AEM. Besides, the chlorine content of O_2 -treated AEM also exhibited an increase, which might be indirectly caused by the content change of the carbon and oxygen. It was inferred that during the O_2 plasma treatment, the conversion of carbonate group (O=C(–O) $_2$) to the volatile products (i.e., CO_2) might lead to the decrease of carbon content [25]. It is known that XPS was used to analyze the relative content of different elements; therefore, the percentage of chlorine might exhibit an increase because of the decrease of the carbon content. Besides, because of the cracks and fragments formed on the surface of O_2 -treated AEM, it was inferred that the chlorine element combined with the quaternary ammonium groups in the O_2 -treated AEM could be detected more, which could cause the increase of the percentage of chlorine with the deposition of the fragments on the surface of O_2 -treated AEM.

3.3. Surface morphology of plasma-treated AEM

It was observed from Fig. 5 that the surface morphology of the plasma-treated AEMs exhibited obvious differences from that of the pristine AEM. Different from the surface of the pristine AEM, some little cracks appeared on the surface of the N_2 -treated AEM, while some big cracks and fragments were also distributed evenly on the surface of the O_2 -treated AEM. Indeed, the dehydration of organic membrane might cause the formation of some cracks on the membrane surface; hence, the pristine AEM and the plasma treated AEMs were dried naturally and pretreated under the same condition

Table 1
Surface elemental compositions of the pristine AEM and the plasma-treated AEMs

	Atomic concentration (%)				Atomic ratio	
	C _{1s}	O _{1s}	N _{1s}	Cl _{2p}	O/C	N/C
Pristine AEM	78.52	13.54	3.16	4.79	0.17	0.04
N_2 plasma-treated AEM	75.65	17.13	3.58	3.64	0.23	0.05
O_2 plasma-treated AEM	65.47	20.68	3.34	10.51	0.32	0.05

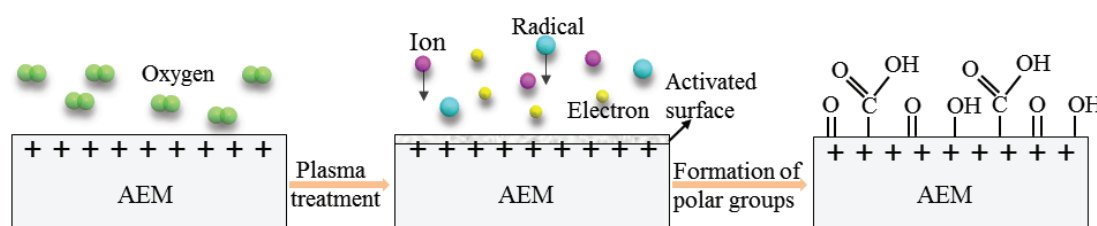


Fig. 4. Schematic diagram of surface functionalization of the AEMs through O_2 plasma treatment.

before observed by SEM; however, it is observed that no cracks appeared on the surface of the pristine AEM; therefore, it is known that the cracks on the surface of the plasma treated AEMs were caused by plasma treatment not the dehydration of membrane. It was inferred that, during the plasma treatment, surface functionalization and etching process of the membrane surface might occur simultaneously or either of the processes might dominate, which would affect the surface morphology of AEMs to different extent. It was reported that nitrogen plasma was not as aggressive as the oxidizing plasmas such as O_2 plasma, hence, the difference of surface morphology between the N_2 - and O_2 -treated AEMs might be caused by the different etching effects. It was inferred that the surface functionalization of N_2 -treated membrane dominated, and the etching effect caused by N_2 plasma was excessively weak to result in the formation of the polymer fragments. However, O_2 plasma treatment caused the surface functionalization of the membranes accompanied by the apparent etching process. The polymer fragments caused by plasma treatment were formed and deposited on the membrane surface. Therefore, the effect of O_2 plasma on the surface morphology was greater than that of the N_2 plasma. The similar processes also occurred during the plasma treatment of polypropylene microporous membrane [12]. Interestingly, the SEM images of plasma treated AEMs in our work were similar to that of homogeneous ion-exchange membranes which were soaked in NaClO solution for a long time, obtained by Garcia-Vasquez et al. [26]. It was found that some holes and cavities were formed on the surface of O_2 -treated AEM, which resembled to the microheterogeneity appeared on the membrane surface of soaked AMX-SB in the NaClO

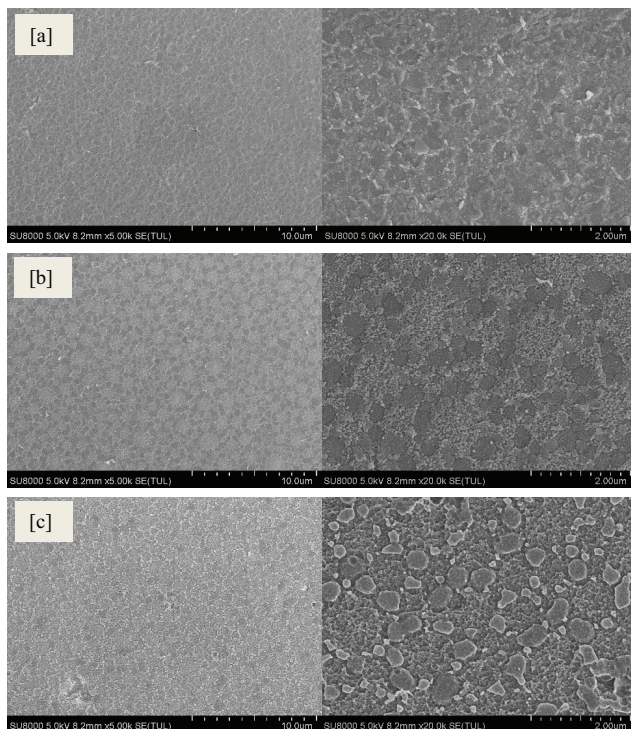


Fig. 5. SEM images with 5,000 \times (left) and 20,000 \times (right) of (a) the pristine AEM; (b) N_2 plasma-treated AEM; and (c) O_2 plasma-treated AEM.

solution. It was inferred that the radicals such as O^{\cdot} , O_2^+ produced by O_2 plasma could lead to the broken of the polymer chain of AEM, but the surface destruction of AMX-SB soaked in the NaClO solution was more evident because of the longer time and the permeation of NaClO into the inside of AMX-SB. The surface morphology of N_2 -treated AEM was similar to that of soaked CMX-SB in NaClO solution, but no evident hole appeared on the surface of N_2 -treated AEM because the N_2 plasma was not such aggressive as O_2 plasma and the plasma treatment acted only on the membrane surface for the short time. Compared with O_2 plasma, the etching effect of N_2 plasma on the AEM was weaker, which led to the different surface morphology changes of the two plasma treated AEMs.

AFM measurement was carried out to further examine the changes of the surface roughness of AEMs and the 3D images are shown in Fig. 6. Surface roughness was characterized in terms of root mean square (R_q) which represented the standard deviation from the mean surface plane, and the maximum roughness (R_{max}) which meant the vertical distance between the highest peaks and the lowest valleys in the image. The R_q value of the pristine AEM, N_2 -treated AEM, and O_2 -treated AEM was 22.2, 22.1, and 23.0 nm, respectively. This result demonstrated the roughness of the membrane surface changed minimally after plasma treatment, which indicated that the sputtering effects were homogenous on the entire surface and changed the membrane surface uniformly. The R_{max} value of the pristine AEM, N_2 -treated AEM,

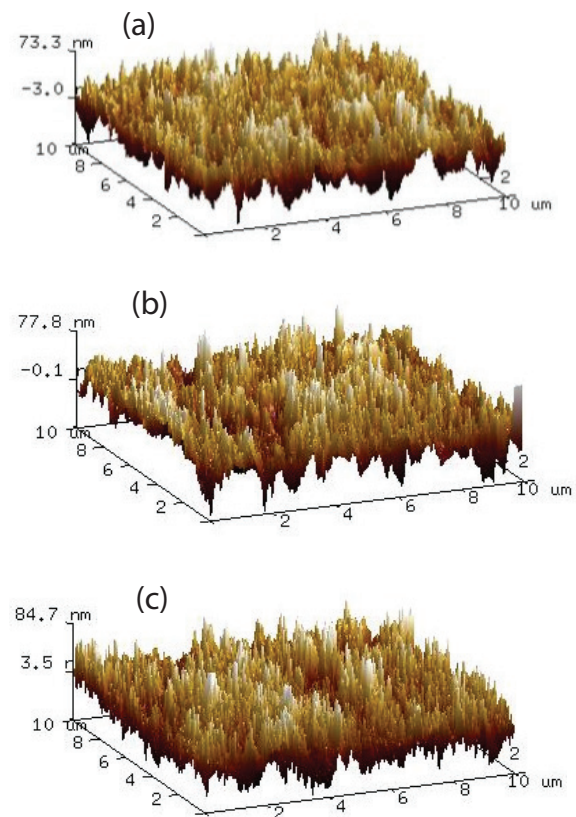


Fig. 6. AFM 3D images (10 $\mu m \times 10 \mu m$) of (a) the pristine AEM; (b) N_2 plasma-treated AEM; and (c) O_2 plasma-treated AEM.

and O₂-treated AEM was 73.3, 77.8, and 84.7, respectively. It was inferred that, compared with N₂ plasma, O₂ plasma had stronger etching effect on the AEM, which caused the R_{max} of the O₂-treated AEM to have an obvious increase.

3.4. Physicochemical properties of plasma-treated AEM

According to the characterization of plasma-treated AEMs by XPS, SEM, and AFM, it was found that the plasma treatment could cause the surface functionalization and had an etching effect on the plasma-treated AEMs; moreover, the type of plasma gases led to the different changes in the physicochemical properties of the different AEMs. The water contact angle, charge density, and electrical resistance of the pristine AEM and the plasma-treated AEMs were characterized and shown in Table 2.




The contact angle values of the pristine AEM, N₂-treated AEM, and O₂-treated AEM were 84.2°, 43.9°, and 63.6°, respectively, with the value of the pristine AEM as the highest. The results indicated that the surface hydrophilicity of the AEMs could be improved by the plasma treatments; moreover, the surface hydrophilicity of the plasma-treated AEM was improved more significantly when N₂ was used as the feed gas. It was inferred that the implanted polar groups, because of the surface functionalization, such as the imide, ester/carboxyl groups were hydrophilic groups, which contributed to the improvement of surface hydrophilicity of the plasma-treated AEMs [15,20]. However, the contact angle of the O₂ plasma-treated AEM was higher than that of the N₂ plasma-treated AEM, it was inferred that the difference of surface hydrophilicity was attributed to the different etching effects caused by feed gases. It was observed that the etching effect of N₂ plasma was minimal, and some little cracks appeared on the surface of N₂-treated AEM. However, the O₂ plasma with strong etching action caused the bigger cracks formed and some fragments distributed evenly on the surface of the O₂-treated AEM, which made the surface of the O₂-treated AEM rugged, to a certain extent, similar to the mastoid structure of lotus leaf. It was known that the special structure of lotus leaf made its surface hydrophobic and some materials with the similar structure of lotus leaf were prepared to obtain the hydrophobic surface [27]. Therefore, it was inferred that the bump structure appeared on the surface of O₂-treated AEM limited the spreading of water droplets and was not beneficial to the decrease of the contact angle, causing the surface of O₂-treated AEM to be less hydrophilic than the N₂-treated AEM.

The surface charges of the pristine AEM and the plasma-treated AEMs were determined by measuring the zeta potential. Table 2 indicates that the zeta potential of the pristine membrane was 7.76 mV, which correlated with the quaternary ammonium groups with positive charge contained in the AEM. The zeta potential of N₂ and O₂ plasma-treated AEMs was -6.2 and -12.4 mV, respectively. It was observed that the zeta potential of the treated membranes became negative after plasma treatments and the type of the feed gas had an different effect on the zeta potential of the treated membranes; besides, the O₂ plasma contributed more in increasing the surface negative charge density of AEM than the N₂ plasma according to the measurements of zeta potential. It was inferred that after plasma treatment, the outermost layer of the membranes changed because of the insertion of the polar groups on the membrane surface. The number of functional groups with a negative charge generated by the O₂ plasma treatment was higher than that generated by the N₂ plasma treatment. It was inferred that the partial functional groups such as amine and amide generated by N₂ plasma were still with positive charge but the functional groups such as ketone, ester, and carboxylic acid were all with negative charge. Therefore, the negative charge density of O₂-treated membrane was higher than that of N₂-treated membrane.

The electrical resistance of the ion-exchange membrane affected the energy consumption and desalination performance of ED, hence, the effect of plasma treatment on the electrical resistance of the membranes was also examined. Table 2 shows that the electrical resistance of the pristine AEM, N₂-treated AEM, and O₂-treated AEM were 3.44, 3.28, and 3.36 Ω·cm², respectively. The results indicated that the electrical resistance of the plasma-treated membranes slightly decreased, which improved ED performance. It was inferred that the outermost layer of plasma-treated AEM was changed, but the bulk properties were almost unaffected after plasma treatment; hence, the electrical resistance of AEM would not change significantly. The polar groups introduced on the surface of the plasma-treated AEM also facilitated the ion migration through the membrane, causing the electrical resistance declined slightly. However, the change of the electrical resistance was almost unaffected by the type of plasma gas.

The contact angle of the N₂- and O₂-treated AEMs was measured as a function of time and shown in Fig. 7. It was observed that the contact angle of the N₂- and O₂-treated AEMs increased gradually with the storage time, and the contact angle value was close to the initial value of the pristine AEM after 6 d. After the plasma treatment, the hydrophilic

Table 2
Water contact angle, zeta potential, and electrical resistance of pristine AEM and plasma-treated AEMs

	Water contact angle (°)	Zeta potential (mV)	Electrical resistance (Ω·cm ²)
Pristine AEM	84.2 ± 2.9 	7.76 ± 0.76	3.44 ± 0.06
N ₂ plasma-treated AEM	43.9 ± 6.5 	-6.2 ± 0.2	3.28 ± 0.06
O ₂ plasma-treated AEM	63.6 ± 1.9 	-12.4 ± 1.1	3.36 ± 0.02

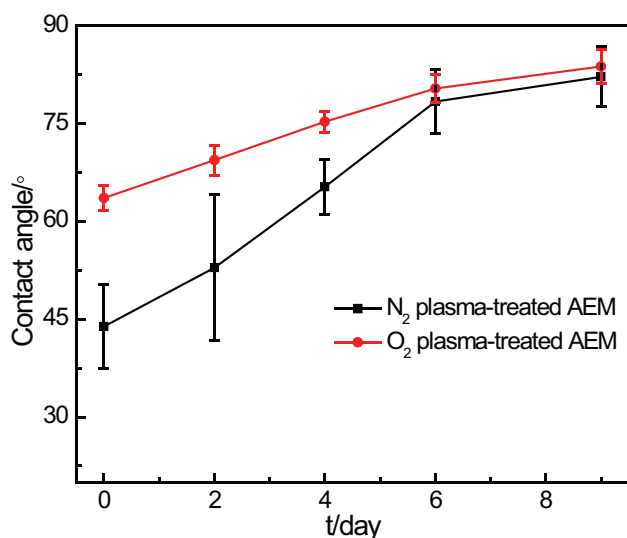


Fig. 7. The change of the contact angle as a function of time for the plasma treated AEMs.

groups were incorporated on the surface of the AEMs, which improved the surface hydrophilicity of the N₂- and O₂-treated AEMs; however, the instability of functional groups caused by plasma treatment made the surface hydrophilicity of the plasma treated AEMs declined with time. Therefore, it is necessary to study further how to keep the high surface hydrophilicity for longer time in the future work.

3.5. ED performance and antifouling property of plasma-treated AEM

Fig. 8(a) shows the electrical conductivity of the solution in the dilute compartment as a function of time. The results showed that the desalination rate of the pristine AEM and the plasma-treated AEMs barely exhibited obvious changes during the same time period. Plasma treatment did not adversely affect the migration of ions (Cl⁻) because the reactions caused by the plasma treatment only occurred on the surface of AEMs almost without changing its bulk properties.

The results of the desalination experiments with 50 mg/L SDBS in the solution in the dilute compartment are presented in Fig. 8(b). The electrical conductivity of the solution without the foulant SDBS in the dilute compartment decreased from approximately 10.5 to roughly 8.5 mS/cm after 90 min of ED desalination when the pristine AEM was used, as indicated in Fig. 8(a). However, when containing 50 mg/L SDBS, the electrical conductivity of the solution in dilute compartment decreased only to ~10.1 mS/cm after 90 min using the pristine AEM, as shown in Fig. 8(b). This finding meant that the transmembrane migration of the ions slowed down because of the membrane fouling from SDBS and membrane fouling occurred at the beginning of the desalination experiment. The desalination rate for the plasma-treated AEM in the presence of SDBS in the dilute compartment was also lower than that without SDBS when the time duration was 90 min. On the basis of Figs. 8(a) and (b), transmembrane migration of the ions through O₂-treated AEM began to slow down

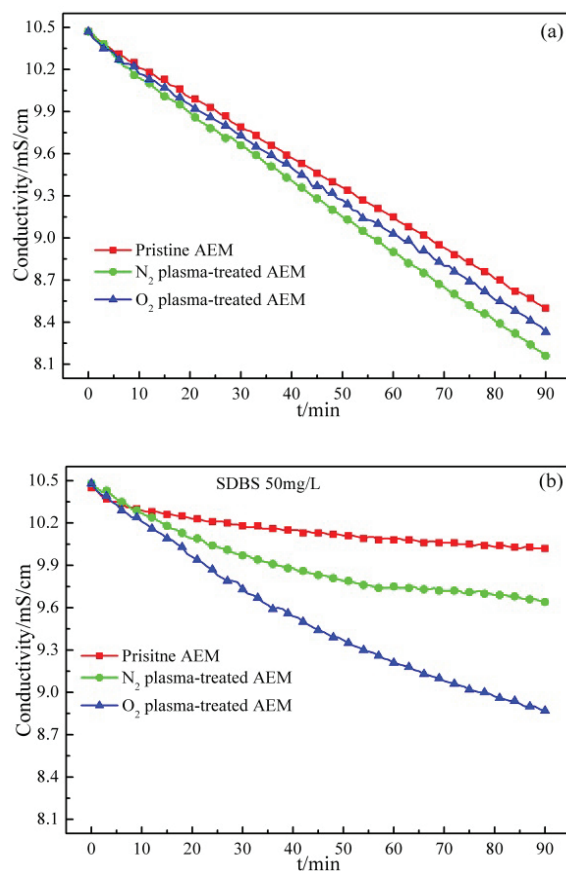


Fig. 8. Electrical conductivity of the solution in dilute compartment during the electro dialysis processes (a) without SDBS and (b) with 50 mg/L of SDBS.

after 50 min, which was obviously superior to that through N₂-treated AEM, and the electrical conductivity of the dilute solution decreased to approximately 8.8 and 9.7 mS/cm for AEM plasma-treated with O₂ and N₂ after 90 min of ED, respectively. These results indicated that the antifouling performance of the plasma-treated AEMs was improved unlike the pristine AEM, and the O₂ plasma-treated AEM exhibited better antifouling performance than the N₂ plasma-treated AEM.

The results of the fouling experiments are shown in Fig. 9. During the fouling experiment using the pristine AEM, the potential difference (ΔE) of the AEM increased significantly with time and ΔE increased to around 3.2 V after 90 min. When the fouling experiment was carried out using N₂ plasma-treated AEM, the ΔE of the AEM increased after approximately 13 min and the final potential difference was roughly 1.5 V. For O₂ plasma-treated AEM, the potential difference was almost unchanged before 50 min during the fouling experiment and ΔE increased slightly to 0.7 V after. The results were consistent with the conclusions obtained from the desalination experiments. However, further work is still needed to improve the stability of the polar groups implanted on the membrane surface for a longer time and higher foulant concentration during ED.

The experimental results indicated that the improvement of the antifouling property of the plasma-treated

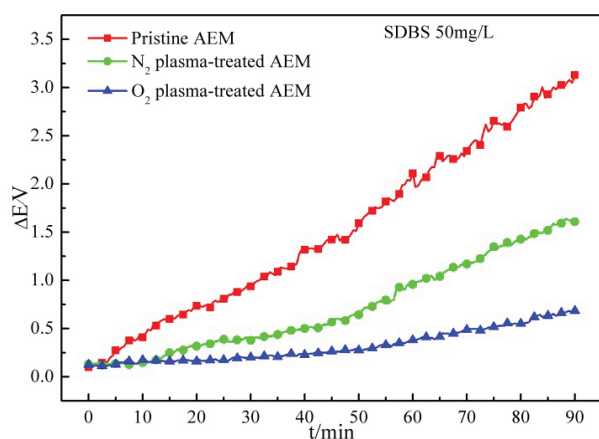


Fig. 9. Potential difference (ΔE) of the pristine AEM and the plasma-treated AEMs in the fouling experiments as a function of time.

AEM resulted from the significant increase of the surface hydrophilicity and surface negative charge density of AEM after plasma treatments, although the surface roughness of AEMs exhibited no obvious changes. SDBS with sulfonic acid group in the feed solution would move to the anode by electromigration and they would enter into the membrane channel or accumulated on the surface of AEMs under a DC electric field. Then, the foulant SDBS could be adsorbed on the membrane surface by the electrostatic interaction because of the opposite charge; moreover, the affinity interaction between the hydrophobic dodecyl chain/benzene ring of SDBS and the membrane matrix would strengthen the adsorption of the foulant on the membrane surface. As surface hydrophilicity of the plasma-treated AEMs increased, the affinity interaction between the foulant SDBS and the membrane matrix would become weakened, which was beneficial to inhibiting the adsorption of SDBS on the membrane surface and then would reduce the fouling effects [9,12]; and the electrostatic repulsion occurred because of the same charge between the outmost layer of the AEM and the foulant SDBS, which would also make the adsorption of the foulants on the membrane surface more difficult. Thus, the antifouling performance of plasma-treated AEMs was improved unlike the pristine AEM. Moreover, O_2 -treated AEM exhibited better antifouling performance than that of the N_2 -treated AEM. It was inferred the increase of the negative charge density of the membrane surface was more beneficial in improving the antifouling performance than the increase of surface hydrophilicity. The result indicated that improving electrostatic repulsion (i.e., increasing membrane surface negative charge density) was more beneficial in reducing the adsorption of the foulants on the membrane than weakening the affinity interaction (i.e., increasing membrane surface hydrophilicity). This result was an apparent difference between the AEM and the other polymeric membranes, such as microporous membrane and RO membrane, only increasing the surface hydrophilicity could significantly improve the antifouling performance [11,28]. O_2 -treated AEM exhibited better antifouling performance for SDBS than N_2 -treated AEM because of the higher surface negative charge density in the real ED system.

4. Conclusions

The AEM was modified by the low-temperature plasma treatment with N_2 and O_2 as feed gases. XPS analysis confirmed that the plasma treatments incorporated the polar groups on the surface of the plasma-treated AEMs, such as the nitrogen-containing groups for N_2 plasma-treated AEM and the oxygen-containing functionalities for O_2 plasma-treated AEM. Additionally, the polar groups variably improved the surface hydrophilicity and surface negative charge density of the plasma-treated AEMs. SEM showed that O_2 plasma caused more evident changes in the surface morphology than N_2 plasma because the etching effect of O_2 was more aggressive. However, the plasma treatment exhibited almost no negative effects on the electrical resistance and ED performance.

The desalination experiments and fouling experiments demonstrated that the antifouling performance of the plasma-treated AEMs improved because of the increase of both surface hydrophilicity and surface negative charge density. The O_2 plasma-treated AEM exhibited better antifouling performance than the N_2 plasma-treated AEM. The antifouling performance and surface properties of the O_2 and N_2 plasma-treated AEMs proved that the increase of surface negative charge density was more critical to improving the antifouling performance than the increase of surface hydrophilicity. Further work is needed to improve the antifouling performance and the stability of surface antifouling layer of plasma-treated AEMs.

Acknowledgments

The financial support from National Natural Science Foundation of China (21076214), Henan science and technology open cooperation project (172106000076), Beijing Natural Science Foundation (8132047) and National water pollution control and management technology major projects (2014ZX07201-011-003) are greatly appreciated.

References

- [1] V. Lindstrand, G. Sundstrom, A.S. Jonsson, Fouling of electro dialysis membranes by organic substances, *Desalination*, 128 (2000) 91–102.
- [2] H. Strathmann, *Ion-Exchange Membrane Separation Processes*, Elsevier, 2004.
- [3] H. Guo, L. Xiao, S. Yu, H. Yang, J. Hu, G. Liu, Y. Tang, Analysis of anion exchange membrane fouling mechanism caused by anion polyacrylamide in electro dialysis, *Desalination*, 346 (2014) 46–53.
- [4] H. Lee, M. Hong, S. Han, J. Shim, S. Moon, Analysis of fouling potential in the electro dialysis process in the presence of an anionic surfactant foulant, *J. Membr. Sci.*, 325 (2008) 719–726.
- [5] H.-J. Lee, J.-H. Choi, J. Cho, S.-H. Moon, Characterization of anion exchange membranes fouled with humate during electro dialysis, *J. Membr. Sci.*, 203 (2002) 115–126.
- [6] J.-S. Park, J.-H. Choi, K.-H. Yeon, S.-H. Moon, An approach to fouling characterization of an ion-exchange membrane using current–voltage relation and electrical impedance spectroscopy, *J. Colloid Interface Sci.*, 294 (2006) 129–138.
- [7] S. Mulyati, R. Takagi, A. Fujii, Y. Ohmukai, T. Maruyama, H. Matsuyama, Improvement of the antifouling potential of an anion exchange membrane by surface modification with a polyelectrolyte for an electro dialysis process, *J. Membr. Sci.*, 417 (2012) 137–143.

- [8] S. Mulyati, R. Takagi, A. Fujii, Y. Ohmukai, H. Matsuyama, Simultaneous improvement of the monovalent anion selectivity and antifouling properties of an anion exchange membrane in an electrodialysis process, using polyelectrolyte multilayer deposition, *J. Membr. Sci.*, 431 (2013) 113–120.
- [9] L. Zou, I. Vidalis, D. Steele, A. Michelmore, S. Low, J. Verberk, Surface hydrophilic modification of RO membranes by plasma polymerization for low organic fouling, *J. Membr. Sci.*, 369 (2011) 420–428.
- [10] Z. Zhao, H. Cao, S. Shi, Y. Li, L. Yao, Characterization of anion exchange membrane modified by electrodeposition of polyelectrolyte containing different functional groups, *Desalination*, 386 (2016) 58–66.
- [11] K.R. Kull, M.L. Steen, E.R. Fisher, Surface modification with nitrogen-containing plasmas to produce hydrophilic, low-fouling membranes, *J. Membr. Sci.*, 246 (2005) 203–215.
- [12] H.-Y. Yu, X.-C. He, L.-Q. Liu, J.-S. Gu, X.-W. Wei, Surface modification of polypropylene microporous membrane to improve its antifouling characteristics in an SBR: N₂ plasma treatment, *Water Res.*, 41 (2007) 4703–4709.
- [13] H.-Y. Yu, L.-Q. Liu, Z.-Q. Tang, M.-G. Yan, J.-S. Gu, X.-W. Wei, Surface modification of polypropylene microporous membrane to improve its antifouling characteristics in an SBR: air plasma treatment, *J. Membr. Sci.*, 311 (2008) 216–224.
- [14] D. Weibel, C. Vilani, A. Habert, C. Achete, Surface modification of polyurethane membranes using RF-plasma treatment with polymerizable and non-polymerizable gases, *Surf. Coat. Technol.*, 201 (2006) 4190–4194.
- [15] D. Wilson, N. Rhodes, R. Williams, Surface modification of a segmented polyetherurethane using a low-powered gas plasma and its influence on the activation of the coagulation system, *Biomaterials*, 24 (2003) 5069–5081.
- [16] S. Sultana, J. Matsui, S. Mitani, M. Mitsuishi, T. Miyashita, Silicon-containing polymer nanosheets for oxygen plasma resist application, *Polymer*, 50 (2009) 3240–3244.
- [17] I. Tepermeister, H. Sawin, X-ray photoelectron spectroscopy study of polymer surface reactions in F₂ and O₂ gases and plasmas, *J. Vac. Sci. Technol., A*, 10 (1992) 3149–3157.
- [18] E. Alkan, E. Kır, L. Oksuz, Plasma modification of the anion-exchange membrane and its influence on fluoride removal from water, *Sep. Purif. Technol.*, 61 (2008) 455–460.
- [19] X.-y. Zhao, Q. Wang, S.-y. Shi, W. Cong, Measurement of area resistance of ion-exchange membrane and its influential factors, *Chin. J. Process Eng.*, 11 (2011) 329–335 (in Chinese).
- [20] Y.-H. Choi, J.-H. Kim, K.-H. Paek, W.-T. Ju, Y.S. Hwang, Characteristics of atmospheric pressure N₂ cold plasma torch using 60-Hz AC power and its application to polymer surface modification, *Surf. Coat. Technol.*, 193 (2005) 319–324.
- [21] J. Fresnais, J.P. Chapel, F. Poncin-Epaillard, Synthesis of transparent superhydrophobic polyethylene surfaces, *Surf. Coat. Technol.*, 200 (2006) 5296–5305.
- [22] C. López-Santos, F. Yubero, J. Cotrino, A.R. González-Elipe, Nitrogen plasma functionalization of low density polyethylene, *Surf. Coat. Technol.*, 205 (2011) 3356–3364.
- [23] C.M. Cepeda-Jiménez, R. Torregrosa-Maciá, J.M. Martí, Surface modifications of EVA copolymers by using RF oxidizing and non-oxidizing plasmas, *Surf. Coat. Technol.*, 174 (2003) 94–99.
- [24] S. Rutherford, D. Do, Review of time lag permeation technique as a method for characterisation of porous media and membranes, *Adsorption*, 3 (1997) 283–312.
- [25] B.D. Tompkins, J.M. Dennison, E.R. Fisher, H₂O plasma modification of track-etched polymer membranes for increased wettability and improved performance, *J. Membr. Sci.*, 428 (2013) 576–588.
- [26] W. Garcia-Vasquez, R. Ghalloussi, L. Dammak, C. Larchet, V. Nikonenko, D. Grande, Structure and properties of heterogeneous and homogeneous ion-exchange membranes subjected to ageing in sodium hypochlorite, *J. Membr. Sci.*, 452 (2014) 104–116.
- [27] H.J. Li, X.B. Wang, Y.L. Song, Y.Q. Liu, Q.S. Li, L. Jiang, D.B. Zhu, Super-“amphiphobic” aligned carbon nanotube films, *Angew. Chem. Int. Ed.*, 40 (2001) 1743–1746.
- [28] M.-G. Yan, L.-Q. Liu, Z.-Q. Tang, L. Huang, W. Li, J. Zhou, J.-S. Gu, X.-W. Wei, H.-Y. Yu, Plasma surface modification of polypropylene microfiltration membranes and fouling by BSA dispersion, *Chem. Eng. J.*, 145 (2008) 218–224.